MODIS-Aqua reveals evolving phytoplankton community structure during the Arabian Sea Northeast Monsoon

P. Jeremy Werdell, Ocean Ecology, NASA GSFC, Collin S. Roesler, Bowdoin College, and Joaquim I. Goes, Lamont Doherty Earth Observatory, Columbia University

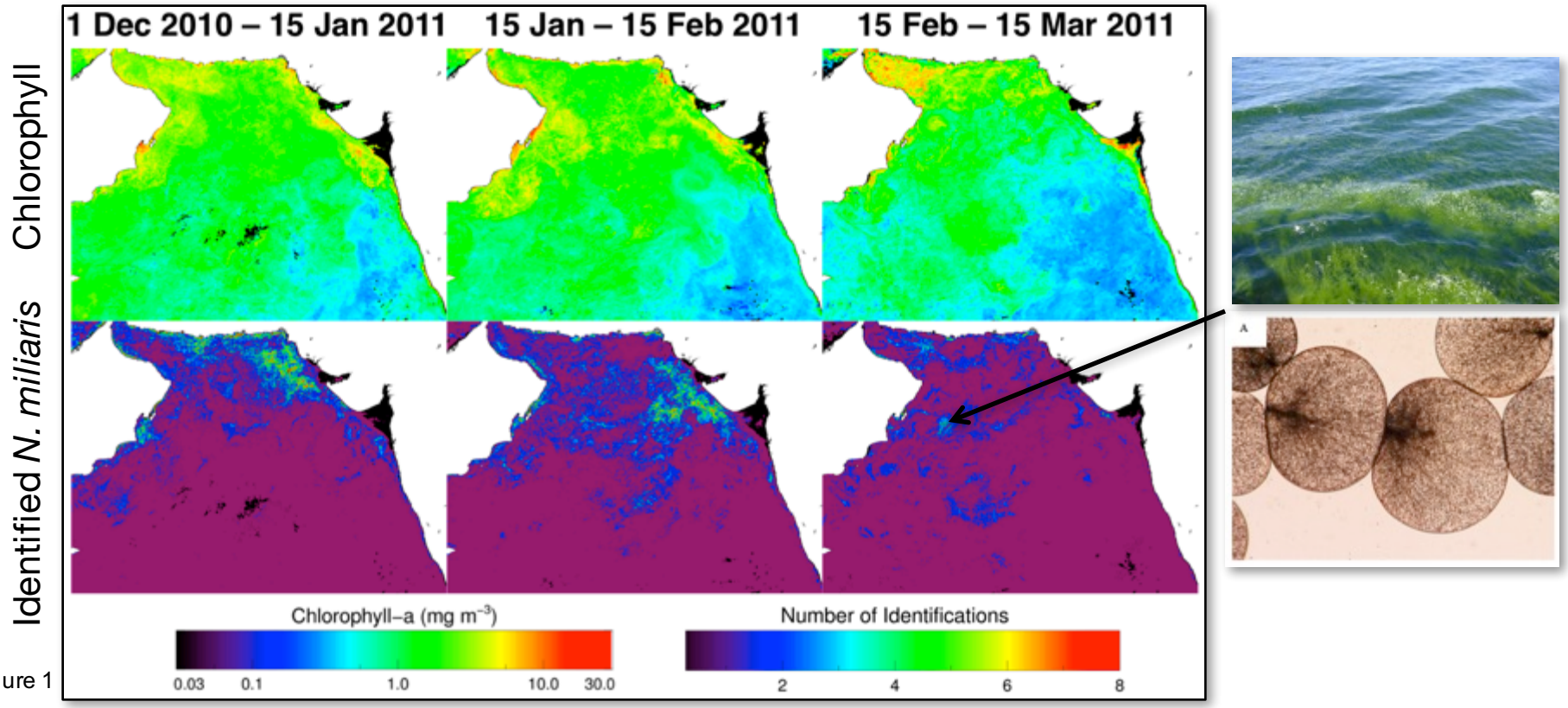

Figure 1

Applying a bio-optical model designed to identify the mixotrophic dinoflagellate *Noctiluca miliaris* to MODIS-Aqua revealed (1) patterns in its spatial distribution not previously seen (including its appearance in places not previously sampled), and (2) the surprising disassociation of total chlorophyll biomass with the presence of *N. miliaris*.

Name: P. Jeremy Werdell, Ocean Ecology, NASA GSFC
E-mail: jeremy.werdell@nasa.gov
Phone: 301-286-1440

References:

P.J. Werdell, C.S. Roesler, and J.I. Goes. Prepared for submission. Remotely search for *Noctiluca miliaris* in the Arabian Sea.

P.J. Werdell, C.S. Roesler, and J.I. Goes, Discrimination of phytoplankton functional groups using an ocean reflectance inversion model, Applied Optics 53, doi:10.1364/AO.53.004833, 2014

P.S. Thibodeau, C.S. Roesler, S.L. Drapeau, S.G.P. Matondkar, J.I. Goes, and P.J. Werdell, Locating Noctiluca miliaris in the Arabian Sea: An optical proxy approach, Limnology and Oceanography 59, doi:10.4319/lo.2014.59.6.2042, 2014

Data Sources: Chlorophyll-a and the absorption coefficients of diatoms and *Noctiluca miliaris* at 443-nm from MODIS-Aqua.

Technical Description of Figures:

Figure 1: Progression of the geographic distribution of total chlorophyll and *Noctiluca miliaris* during the boreal Winter of 2010-2011 at 2 km resolution. Top row shows chlorophyll-a (mg m^{-3}) from MODIS-Aqua. Bottom row shows *N. miliaris* identified based on thresholds of the absorption coefficients of diatoms and *N. miliaris* at 443-nm from MODIS-Aqua. Regions of white and black indicate land and no satellite retrievals (including model failure). Three sequential time periods encompassing the Northeast Monsoon season are shown from left to right: 1 Dec 2010 to 15 Jan 2011, 15 Jan to 15 Feb 2011, and 15 Feb to 15 Mar 2011. The images of a surface bloom of *N. miliaris* (top right) and its cells (bottom right) are courtesy of J.I. Goes and H.R.G. Gomes (Columbia University).

Scientific significance, societal relevance, and relationships to future missions: Changes in phytoplankton community composition in the northern Arabian Sea during the annual Northeast Monsoon have been linked to the appearance of the mixotrophic dinoflagellate *Noctiluca miliaris*. This emergence is ultimately expected to alter predator-prey relationships of higher trophic levels, and thus, carbon export to the deep ocean. Records of *in situ* counts of *N. miliaris* only first appear in the late 1990s and remain discontinuous. The daily imagery provided by satellite ocean color instruments, however, provide time-series of sufficient length to allow retrospective analyses. Applying a bio-optical model designed to identify *N. miliaris* to MODIS-Aqua revealed (1) patterns in its spatial distribution not previously seen (including its appearance in places not previously sampled), and (2) the surprising disassociation of total chlorophyll biomass with the presence of *N. miliaris*. This MODIS-Aqua imagery provided substantial insight into *N. miliaris* (and other phytoplankton) dynamics that could not have been achieved by *in situ* sampling alone and pointed to specific places and times for targeted future studies.

Harmonizing Landsat and Sentinel-2 Reflectances for Better Land Monitoring

Jeffrey Masek, Biospheric Sciences, NASA GSFC, Eric Vermote, Terrestrial Information Systems, NASA GSFC, Belen Franch, University of Maryland, Jean-Claude Roger, University of Maryland, Sergii Skakun, University of Maryland, Junchang Ju, USRA, NASA GSFC, Martin Claverie, University of Maryland, NASA GSFC, Jennifer Dungan, NASA ARC

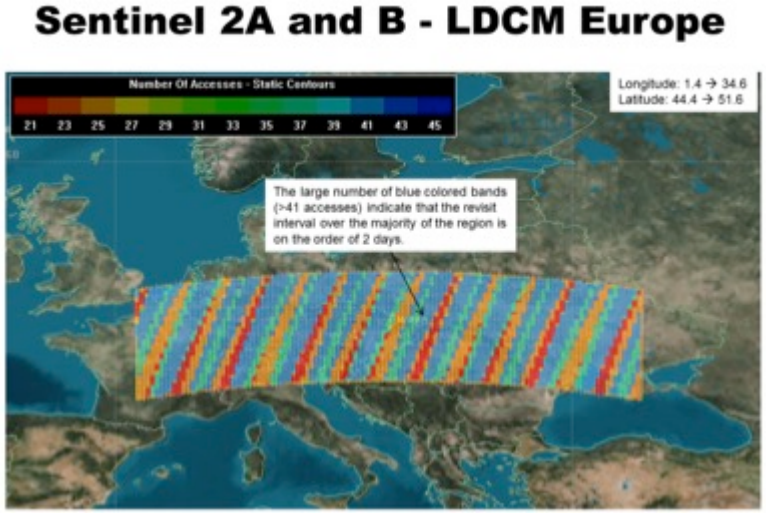

Figure 1

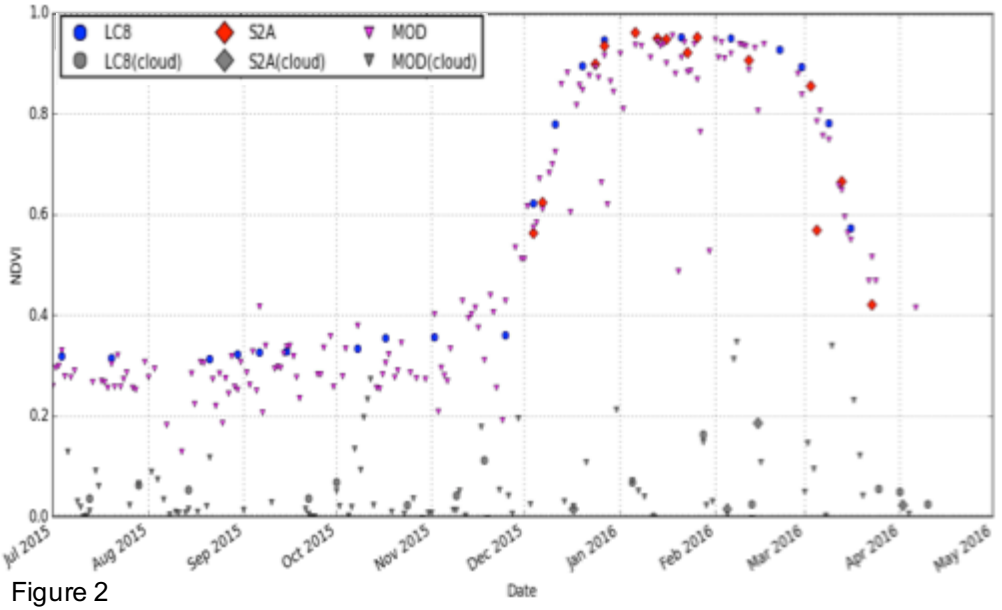

Figure 2

When combined, Landsat and ESA Sentinel-2 observations can provide 2-4 day coverage for the global land area. A collaboration among NASA GSFC, University of Maryland, and NASA Ames has developed a processing chain to create seamless, "harmonized" reflectance products using standardized atmospheric correction, BRDF adjustment, spectral bandpass adjustment, and gridding algorithms. These products point the way to a "30-m MODIS" capability for agricultural and ecosystem monitoring by leveraging international sensors.

Name: Jeff Masek, Biospheric Sciences, NASA GSFC
E-mail: Jeffrey.G.Masek@nasa.gov
Phone: 301-614-6629

References:
N/A

Data Sources: Surface reflectance products derived from Landsat-8 OLI, Sentinel-2 MSI, and Terra/Aqua MODIS.

Technical Description of Figures:
Figure 1: Acquisition frequency over mid-latitudes (Europe) expected from two Sentinel-2 satellites (Sentinel-2a,b) combined with Landsat-8. Blue-colored areas indicate an expected frequency of at least one observation every two days (figure courtesy Brian Killough, LaRC).
Figure 2: Seasonal cycle of greenness (NDVI) derived from Landsat (blue) and Sentinel-2a (red) harmonized reflectance data for a single agricultural field in Argentina. The NDVI values closely track the more frequent MODIS (small red triangle) acquisitions. Cloud-contaminated observations are shown in grey, and typically have low apparent NDVI values (figure courtesy Belen Franch, UMD).

Scientific significance, societal relevance, and relationships to future missions: Monitoring patch-scale vegetation dynamics, particularly for agricultural regions, requires both fine spatial resolution and <8-day temporal frequency. While it is difficult for a single satellite program (such as Landsat) to satisfy these goals, harmonizing multiple international sources of data can provide a cost-effective pathway to such a "30-m MODIS" capability. The Sentinel-2 (ESA) and Landsat (NASA/USGS) are complementary systems, with similar spectral bands and spatial resolution. Work by NASA GSFC, ARC, and University of Maryland has created a processing chain to create harmonized surface reflectance time series using data from both sensors. The processing chain applies a common atmospheric correction based on the MODIS MCD09 approach, and corrects for differences in view angle, spectral bandpass, and gridding. These harmonized 30-m reflectance products can be used to monitor field-scale agricultural productivity and crop type in support of the GEO Global Agricultural Monitoring (GEO-GLAM) initiative.

AERONET Version 3 Release—Providing significant improvements for multi-decadal global aerosol database and near real-time validation

Brent Holben, Ilya Slutsker, David Giles, Thomas Eck, Alexander Smirnov, Aliaksandr Sinyuk, Joel Schafer

Mikhail Sorokin, Jon Rodriguez, Jason Kraft, Amy Scully, Biospheric Sciences Laboratory

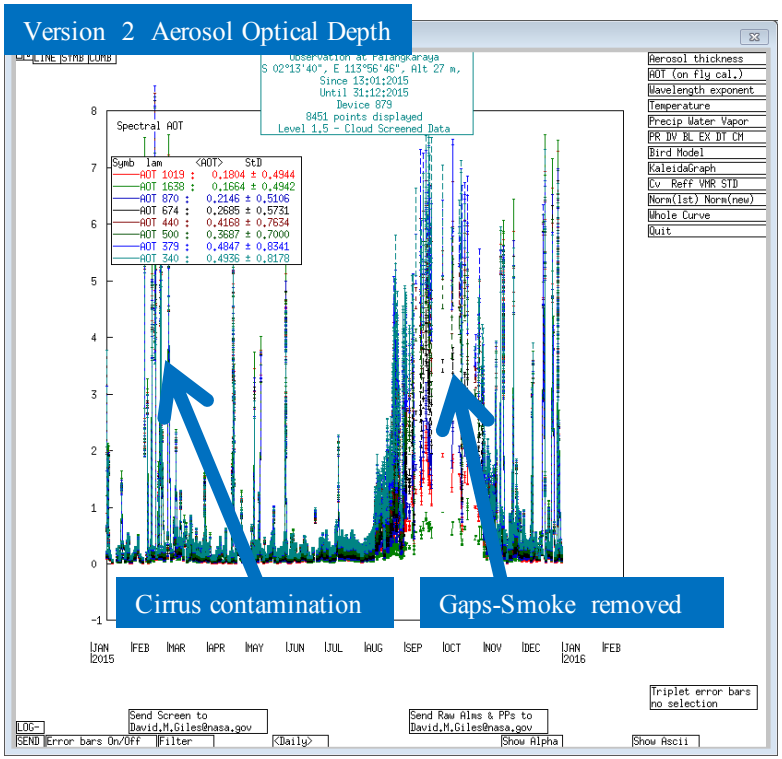

Figure 1

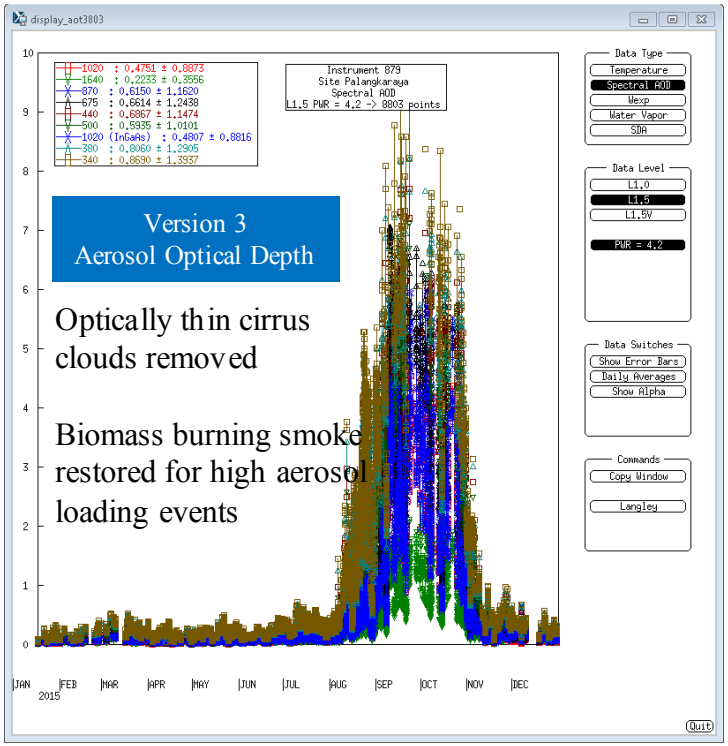

Figure 2

Aerosols are highly variable in space, time and properties. Global assessment from satellite platforms and model predictions rely on validation from AERONET, a highly accurate ground-based network. Ver. 3 represents a significant improvement in accuracy and quality.

Name: Brent Holben, Biospheric Sciences Laboratory, NASA GSFC
E-mail: brent.n.holben@nasa.gov
Phone: 301-614-6658

References:

2014, Eck, T. F., Holben, B. N., Reid, J. S., Arola, A., Ferrare, R. A., Hostetler, C. A., Crumeyrolle, S. N., Berkoff, T. A., Welton, E. J., Lolli, S., Lyapustin, A., Wang, Y., Schafer, J. S., Giles, D. M., Anderson, B. E., Thornhill, K. L., Minnis, P., Pickering, K. E., Loughner, C. P., Smirnov, A., and Sinyuk, A.: Observations of rapid aerosol optical depth enhancements in the vicinity of polluted cumulus clouds, Atmos. Chem. Phys., 14, 11633-11656, doi: 10.5194/acp-14-11633-2014, 2014.

Schafer, J. S., et al. (2014), Intercomparison of aerosol single-scattering albedo derived from AERONET surface radiometers and LARGE in situ aircraft profiles during the 2011 DRAGON-MD and DISCOVER-AQ experiments, J. Geophys. Res. Atmos., 119, doi:10.1002/2013JD021166.

2012, Giles, D. M., B. N. Holben, T. F. Eck, A. Sinyuk, A. Smirnov, I. Slutsker, R. R. Dickerson, A. M. Thompson, and J. S. Schafer (2012), An analysis of AERONET aerosol absorption properties and classifications representative of aerosol source regions, J. Geophys. Res., 117, D17203, doi:10.1029/2012JD018127.

2012, Sinyuk, A., B. N. Holben, A. Smirnov, T. F. Eck, I. Slutsker, J. S. Schafer, D. M. Giles, and M. Sorokin (2012), Assessment of error in aerosol optical depth measured by AERONET due to aerosol forward scattering, Geophys. Res. Lett., 39, L23806, doi:10.1029/2012GL053894.

2000, Smirnov A., B.N.Holben, T.F.Eck, O.Dubovik, and I.Slutsker, 2000: Cloud screening and quality control algorithms for the AERONET database, Rem.Sens.Env., 73, 337-349.

1998, Holben B.N., T.F.Eck, I.Slutsker, D.Tanre, J.P.Buis, A.Setzer, E.Vermote, J.A.Reagan, Y.Kaufman, T.Nakajima, F.Lavenu, I.Jankowiak, and A.Smirnov, 1998: AERONET - A federated instrument network and data archive for aerosol characterization, Rem. Sens. Environ., 66, 1-16.

Data Sources: All data are collected by the federated partners of the AERONET program that contribute to AERONET's public domain database.

Figure 1: *This figure shows the V2 screened aerosol optical depth (AOD) data for 2015 in Borneo which is typically characterized by low AOD most of the year but in 2015 a severe biomass burning season enhanced by a very strong el Nino produced extraordinarily high AOD in August through November reducing visibility to a few hundred meters for weeks. Note the high spikes throughout the year due to very stable cirrus clouds that are very difficult to remove from the aerosol data. During very heavy smoke events, the radiometric signal is weak such that many gaps in the data can occur.*

Figure 2: *The same 2015 Borneo dataset but screened with Version 3 that does a superior job removing cirrus contaminated data while restoring data from the strong extinction caused by heavy smoke in August through November. Improved data corrections, cloud screening and quality assurance algorithms have been developed, revised and tested over the past three years and V3 data are now available at http://aeronet.gsfc.nasa.gov.*

Version 3 processing is anchored to a completely revised data management system known as 'Demonstrat'. With the growth to over 600 federated sites distributed world wide, AERONET required a more efficient system of calibration, processing, archive and distribution to serve NASA, AERONET's collaborators and the aerosol community.

The sun and sky scanning spectral radiometer , AKA cimel*, is standard equipment across the network, being largely unchanged for more than 23 years. Imposing standardization of the equipment, calibration, processing, and all phases of data management combined with an open data policy has allowed the project to serve the global community, provide data for fundamental research and serve as a model for other NASA networks.*

Scientific significance, societal relevance, and relationships to future missions: AERONET is the world standard for ground-based remote sensing of aerosol properties for it's accuracy, availability and global distribution. By the nature of the physics, ground-based aerosol measurements are more accurate than model estimates and satellite retrievals, thus AERONET has become the world validation reference for all modeling efforts and satellite systems. Version 3 by improving the accuracy moves our scientific understanding of aerosol properties, distributions and processes forward. The near real-time data available under Version 3 is a critical component of many aerosol related NASA field missions, most recently KORUS-AQ in S. Korea. The value to the community is tracked in the number of citations of the Holben et al. 1998 AERONET reference paper that currently exceeds 4000.

MABEL photon-counting laser altimetry data in Alaska for ICESat-2 simulations and development

Kelly Brunt, Cryospheric Sciences, NASA GSFC, T.A. Neumann, Cryospheric Sciences, NASA GSFC, J.M. Amundson, University of Alaska Southeast, J.L. Kavanaugh, University of Alberta, M.S. Moussavi, CIRES, NSIDC, K.M. Walsh, Cryospheric Sciences, NASA GSFC, W.B. Cook, Mesoscale Atmospheric Processes, NASA GSFC, & T. Markus, Cryospheric Sciences, NASA GSFC

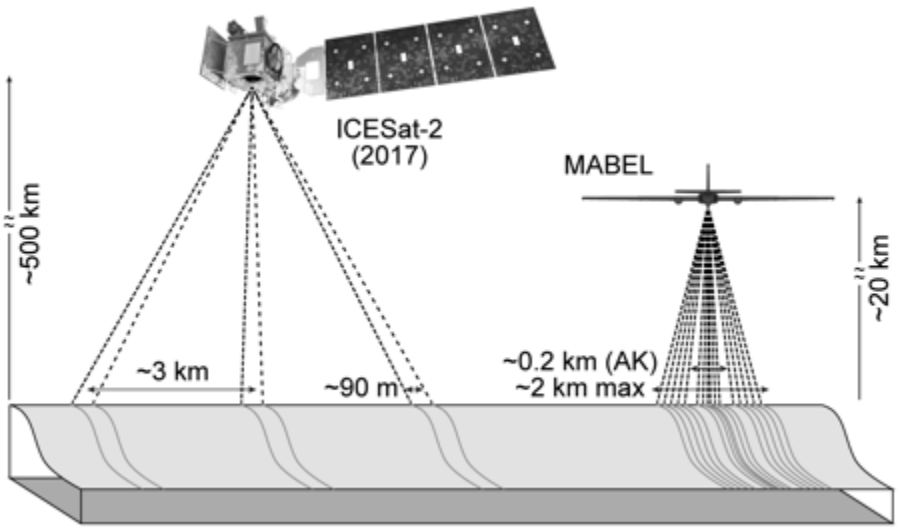

Figure 1

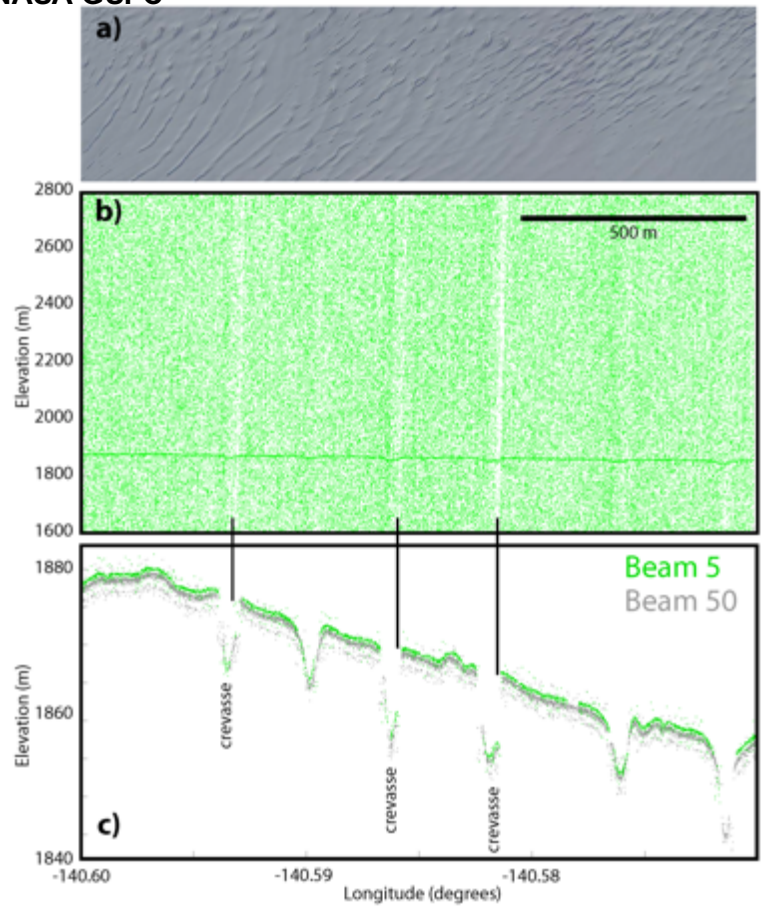

Figure 2

MABEL maps Alaskan crevasses in detail, using ~50% of the expected along-track ATLAS signal-photon densities over summer ice sheets.
ICESat-2 along-track data density, and spatial data density due to the multiple-beam strategy, will provide a new dataset to mid-latitude alpine glacier researchers.

Name: Kelly Brunt, Cryospheric Sciences, NASA GSFC
E-mail: kelly.m.brunt@nasa.gov
Phone: 301-286-5943

References:

This research '**MABEL photon-counting laser altimetry data in Alaska for ICESat-2 simulations and development**' will appear in *The Cryosphere,* 2016.

Data Sources: NASA ICESat-2 MABEL data: (http://icesat.gsfc.nasa.gov/icesat2/data/mabel/mabel_docs.php); Landsat-8 OLI data; WorldView-2 imagery; in situ GPS data on icefields.

Technical Description of Figures:

Figure 1: Schematic ICESat-2 and MABEL beam geometry (dashed lines) and reference ground tracks (grey lines along ice-sheet surface). Each ICESat-2 beam pair consists of a strong and a weak beam (as indicated by the dash difference) for energy considerations. MABEL allows for beam-geometry changes with a maximum ground spacing of ~2 km at 20 km; for the 2014 AK deployment, the maximum ground spacing was 0.2 km (after Brunt et al., 2014).

Figure 2: MABEL camera and photon data over a heavily crevassed section of the Bagley Icefield, from the 16 July 2014 flight. (a) Stitched MABEL camera images. (b) MABEL signal and background photons for a 1200 m range that includes the glacier surface. (c) MABEL signal photons, indicating both the surface and the bottoms of crevasses.

Scientific significance, societal relevance, and relationships to future missions: MABEL is an ICESat-2 data simulator; results from the 2014 Alaska deployment suggest that the dense along-track sampling interval and narrow across-track beam spacing of MABEL (and therefore ATLAS) will provide a level of detail of mountain glaciers that has previously not been achieved from satellite laser altimetry.

Hydrological Impacts from Fire-Induced Surface Albedo Darkening in Africa

Manika Gupta, Hydrological Sciences, NASA GSFC and USRA,
John D. Bolten, Hydrological Sciences, NASA GSFC,
Charles Gatebe and Charles Ichoku, Biospheric Sciences, NASA GSFC

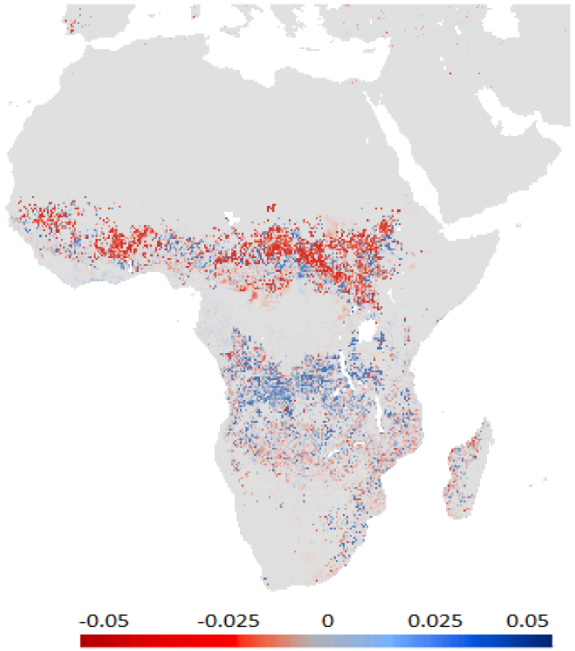

Albedo Change

Figure 1

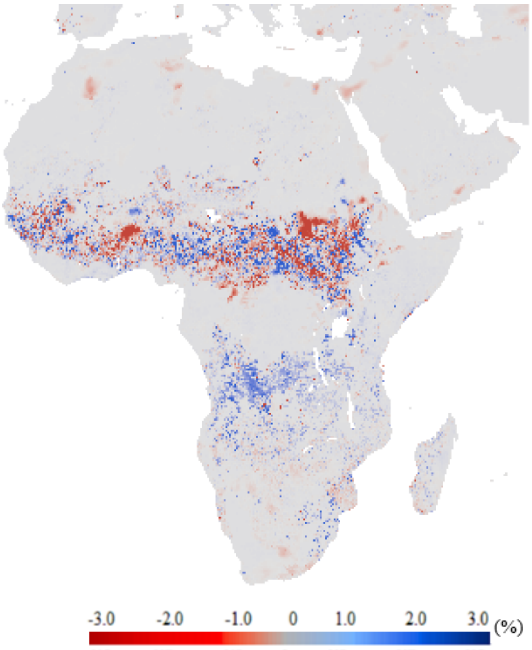

Soil Moisture Change

Figure 2a

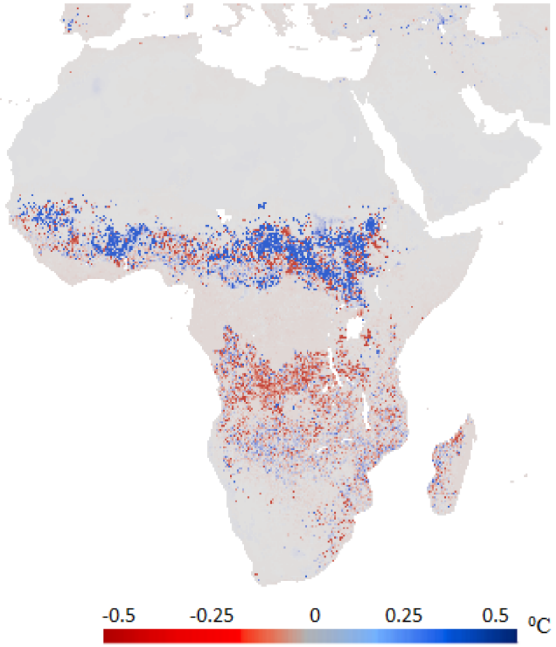

Surface Temperature Change

Figure 2b

Burning of biomass as observed by satellites causes a change in albedo that leads to a 1-3% decrease in soil moisture and up to a 1ºC increase in surface temperature.

Name: Manika Gupta, Hydrological Sciences, NASA GSFC and USRA
E-mail: manika.gupta@nasa.gov
Phone: 301-286-3951

References:

Gupta, M., Bolten, J. D., Gatebe, C., and Ichoku, C., Regional Land Surface Hydrology Impacts from Fire-Induced Surface Albedo Darkening in Africa, Remote Sensing of Environment (In review)

Gatebe, C.K., Ichoku, C.M., Poudyal, R., Román, M.O., Wilcox, E., 2014. Surface albedo darkening from wildfires in northern sub-Saharan Africa. Environmental Research Letters 9, 065003. doi:10.1088/1748-9326/9/6/065003

Data Sources:

Modelled Products – soil moisture estimates obtained from NASA-LIS integrated Catchment Land Surface Model (CLSM)
Earth observation datasets – MODIS burned area product (MCD45A1), MODIS leaf area index, and MODIS land surface temperature and Greenness Vegetation Fraction (GVF) provided by NESDIS

Technical Description of Figures:

Figure 1: This figure illustrates the difference in mean albedo change for the modified run (with static albedo) with the control run (with modified albedo) for the period 2003-2010 due to fire events occurring

Figure 2a: This figure illustrates the difference in mean of soil moisture for the modified run with the control run for the period 2003-2010 using the Catchment Land surface Model (CLSM) and demonstrates a nearly 1-3% decrease in soil moisture during January after the fires in Dec-Jan.

Figure 2b: This figure illustrates the difference in mean of surface temperature for the modified run with the control run for the period 2003-2010 using the Catchment Land Surface Model (CLSM) and demonstrates a nearly 1^{o}C increase in surface temperature in January for the fires occurring in Dec-Jan.

Scientific significance, societal relevance, and relationships to future missions: Most land surface models do not adequately reflect changes in land surface water and energy cycle fluxes and states from land surface disturbances such as fire because they utilize climatologically-based biophysical parameters. These biophysical parameters are usually determined using built-in lookup tables or have been averaged on a monthly basis using multiple years' worth of earth observation products. However, large scale events such as fires need to be better represented, as they have a direct impact on the hydrological fluxes of a region. The current study employs satellite-observed changes in albedo. We have investigated how the Catchment Land Surface Model simulates hydrological and energy fluxes based on estimated change of surface albedo due to fires over different land cover types. We tested a new simple parameterization approach for the soil albedo and compared with observed MODIS-based land surface temperature. Since surface albedo is a key element of the surface energy balance, it is shown to drive the surface energy and hydrological cycles in the simulations for the eight-year period of study (2003-2010). This approach can be very valuable for climate studies, particularly in regions where surface observational data are scarce.

How Universal Is the Relationship between Remotely Sensed Vegetation Indices (VI) and Crop Leaf Area Index (LAI)?

Yanghui Kang, Mutlu Özdoğan, Samuel C. Zipper (U.Wisconsin), Miguel Román
Terrestrial Information Systems, NASA GSFC

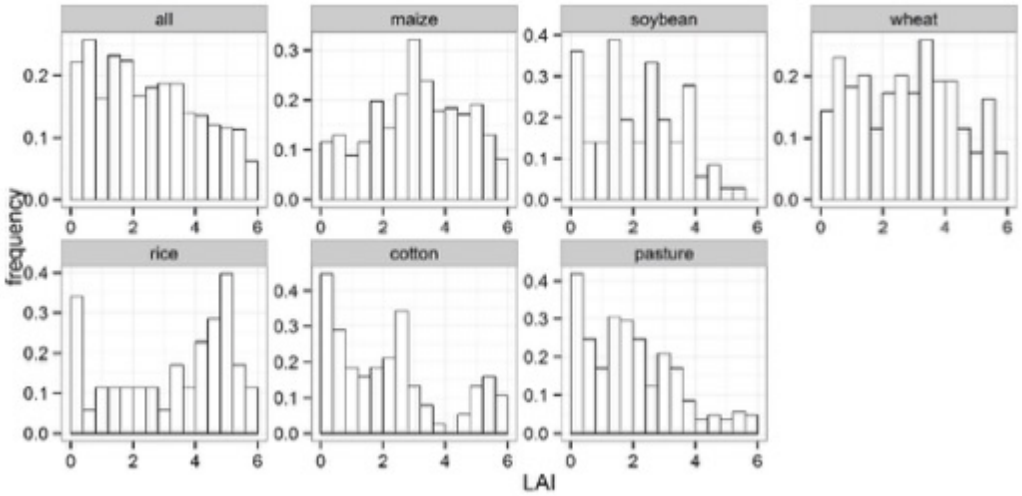

Figure 1

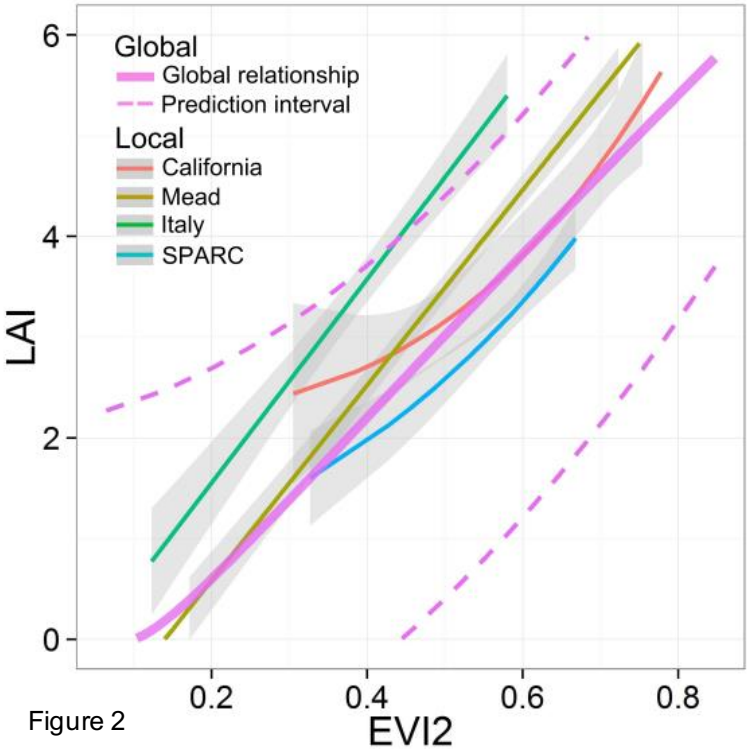

Figure 2

Global LAI-VI relationships are statistically significant, crop-specific, and mostly non-linear. This research enables the operationalization of large-area crop modeling and, by extension, has relevance to both fundamental and applied agroecosystem research.

Name: Miguel O. Román, NASA/GSFC, Code 619
E-mail: Miguel.O.Roman@nasa.gov
Phone: 301-614-5140, 301-614-5498

References:

Kang Y., Özdoğan M., Zipper S., M. O. Román, et al., **How Universal Is the Relationship between Remotely Sensed Vegetation Indices and Crop Leaf Area Index? A Global Assessment**, *MDPI Remote Sensing, doi:10.3390/rs8070597*

Data Sources: A global dataset of 1,459 quality-controlled in-situ crop Leaf Area Index (LAI) measurements were combined with Landsat TM/ETM+ satellite images to derive statistical relationships between LAI and five different Vegetation Indexes (VI), including Simple Ratio (SR), Normalized Difference Vegetation Index (NDVI), two versions of the Enhanced Vegetation Index (EVI and EVI2), and Green Chlorophyll Index (CI_{Green}). We also used the MODIS Collection V005 Nadir BRDF-adjusted reflectance (NBAR) product (MCD43A4) to produce LAI maps using the global LAI-VI relationships. Landsat products were downloaded from USGS Global Visualization Viewer (Glovis) website (http://glovis.usgs.gov). MODIS products were downloaded from the NASA Level 1 and Atmosphere Archive and Distribution System (LAADS) website (https://ladsweb.nascom.nasa.gov/).

Technical Description of Figures:

Figure 1: Frequency distribution of the global in-situ LAI dataset organized by crop types. The distribution of LAI values is positively skewed. Each crop type has a full range of LAI values (from less than 0.12 to more than 5.5 m^2/m^2), which nevertheless distribute differently. The distribution for maize is approximately unimodal, with a peak in the middle (~3 m^2/m^2), and the distribution for pasture is positively skewed. For soybean, wheat, rice, and cotton, the distribution is not as clear or in some cases multimodal.

Figure 2: Local LAI-EVI2 relationships of maize for four major sites compared to the global maize relationship. The thin colored lines are the best-fit functions for each site. The thick solid rose-colored line refers to the global relationship, with dashed rose line being the prediction interval. Gray shaded areas are the 95% confidence intervals. The trend of site-specific relationships are similar to the global relationship, but each relationship has a unique shape and location in the LAI-EVI2 space, leading to bias when using one curve in a different location.

Scientific significance, societal relevance, and relationships to future missions: This work is the first to compile a large dataset of crop LAI and VIs, and analyze the universality and diversity of the LAI-VI relationships globally. These findings not only support the Committee on Earth Observation Satellite's Land Product Validation framework for the validation of remote sensing LAI products, but also contribute to a greater community of users that are interested in producing long time series of LAI records; but do not have access to measured LAI data. The global LAI-VI relationships support the production of large scale fine resolution (30m) LAI maps, which are essential for agricultural applications, especially in regions where crop fields are relatively small. With the successful launch and operation of Landsat-8 and Sentinel-2 satellites, this synthesis can serve as a model for the assessment of terrestrial essential climate variables and key biospherical processes happening at the characteristic scales of vegetation change (e.g., above ground biomass, primary production (NPP), evapotranspiration, and crop yields). The easy accessibility, low cost, and the long historical coverage and continuity of the Landsat-8 and Sentinel-2 missions also render our findings useful to future scientific, governmental, and commercial applications. Finally, as more and more medium to high resolution sensors become available with additional narrow spectral bands (e.g., FLEX and HyspIRI), i.e., the red edge band, great opportunities exists to establish efficient models for global LAI estimation with various hyperspectral VIs.